Journal of Organometallic Chemistry, 213 (1981) 125--137
Elsevier Sequoia S.A., Lausanne — Printed in The Netherlands

THE ROLE OF METAL CLUSTER INTERACTIONS IN THE PROTON-INDUCED REDUCTION OF CO. THE CRYSTAL STRUCTURES OF [PPN][$HFe_4(CO)_{12}C$] AND $HFe_4(CO)_{12}(\eta^2$-$COCH_3)$ *

E.M. HOLT

Department of Chemistry, Oklahoma State University, Stillwater, Oklahoma 74078 (U.S.A.)

K.H. WHITMIRE and D.F. SHRIVER

Department of Chemistry, Northwestern University, Evanston, Illinois 60201 (U.S.A.)

(Received February 6th, 1981)

Summary

The isolation and crystal structure of the iron carbonyl complex [PPN]-[$HFe_4(CO)_{12}C$] (I) from the reaction of [PPN]$_2$[$Fe_4(CO)_{13}$] and HSO_3CF_3 shows it to be a carbide complex. The possible role of the carbide species in the proton-induced reduction of CO is discussed. The structurally similar complex (μ-H)$Fe_4(CO)_{12}(\eta^2$-$COCH_3)$ (II) has also been prepared and its crystal structure determined. Both I and II contain carbon atoms bonded to four irons in a butterfly arrangement. In both, the hydride bridges the two c_{m3} (metal connectivity of three) iron atoms.

Introduction

Recently, we described the proton-induced reduction of a CO ligand in a four-iron metal cluster [1]. In this reaction a proton acid serves as the source of hydrogen nuclei and the metal cluster as an electron source to convert CO to CH_4 and H_2O, eq. 1.

$$Fe_4(CO)_{13}^{2-} \xrightarrow{H^+} CH_4 + H_3O^+ + CO + Fe^{2+} + \text{iron clusters} \quad (1)$$

Isotope tracer and X-ray crystal structure determinations for the proton-induced reaction of an analogous species, $Fe_4(CO)_{12}(COCH_3)^-$, implicates the CO in the $COCH_3^+$ ligand as the site of reduction [2]. The inferences from that study were that an η^2-COH ligand is formed and subsequently reduced to CH_4, Scheme 1.

* Dedicated to the memory of Professor Paolo Chini.

0 022-328X/81/0000—0000/$02.50,

SCHEME 1

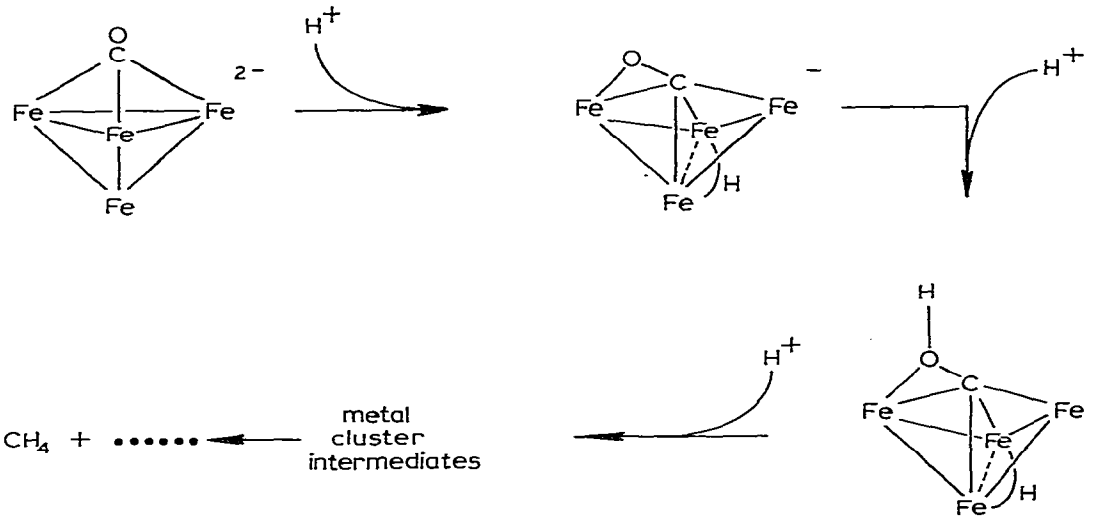

In the present paper we describe the detection of the previously reported [3,4] $HFe_4(CO)_{12}(\eta^2\text{-}CH)$ as an apparent metal cluster intermediate in this reaction. In addition we discuss the detailed structural changes in the cluster which appear to facilitate the CO reduction.

Experimental

Solvents and reagents were dried and distilled using standard methods and stored under inert atmosphere. Infrared spectra were obtained on a Perkin-Elmer 399 or 283 spectrometer, and ^1H NMR measurements were made on a Perkin-Elmer R20B. Calcium fluoride windowed cells were used for the determinations of IR spectra in HSO_3CF_3 solution. Mass spectra were obtained on a Hewlett-Packard 5985 using 20 eV electron impact.

[PPN][$HFe_4(CO)_{12}C$]

To 1 gram of $[PPN]_2[Fe_4(CO)_{13}]$ [PPN = μ-nitridobis(triphenylphosphorus)] at −196°C 2 ml of HSO_3CF_3 was slowly added under an inert atmosphere. The mixture was allowed to warm to room temperature, stirred for 1 h and then extracted with cyclohexane. After removal of cyclohexane under vacuum, the residue was dissolved in methanol. Upon cooling, this solution yielded dark red-black crystals; C, H, N analyses were satisfactory. IR (KBr pellet) 2000(sh), 1985vs, 1975s, 1933s. A crystal of approximate dimensions 0.5 × 0.15 × 0.3 mm was sealed in a glass capillary and mounted on an automatic diffractometer. Unit cell dimensions (Table 1) were determined by least-squares refinement of the angles observed during standard alignment procedures.

(μ-H)$Fe_4(CO)_{12}(\eta^2$-CH)

To a solution of HSO_3CF_3 and $[PPN]_2[Fe_4(CO)_{13}]$, prepared as above, was added ca. 50 ml hexane. From the dark brown-black hexane solution, the sol-

TABLE 1

CRYSTAL DATA

	I	II
Formula	$C_{49}H_{31}Fe_4NO_{12}P_2$	$C_{14}H_4Fe_4O_{13}$
Mol. wt.	1079.96	603.54
Space group	$P\bar{1}$	$P\bar{1}$
Systematic absences	none	none
a (Å)	12.101(7)	9.135(2)
b (Å)	12.942(7)	9.313(2)
c (Å)	15.592(3)	14.759(4)
α (°)	91.323(2)	97.13(2)
β (°)	90.189(2)	99.32(2)
γ (°)	100.789(2)	124.15(2)
V (Å^3)	2397.9	989.4
D_{cal} (g cm^{-3})	1.49	2.02
Z	2	2
μ(Mo-K_α) (cm^{-1})	13.49	30.08
F(000)	1138	592
Observed data ($I > 3\sigma(I)$)	2953	3104

vent was removed in vacuo. The product was dissolved in CD_2Cl_2 and identified as (μ-H)$Fe_4(CO)_{12}(\eta^2$-CH) by ^{1}H NMR, δ = —1.31 ppm, 1 H; —27.9 ppm, 1 H [3]. Elemental analyses for C and H were satisfactory. IR: 2095w, 2045vs, 2027s, 2015s, 1980m cm^{-1}. The compound was also synthesized by the method of Tachikawa and Muetterties [3].

Reaction of HSO_3CF_3 with (μ-H)$Fe_4(CO)_{12}(\eta^2$-CH)

Following the procedure outlined above a mixture of 0.13 g (μ-H)$Fe_4(CO)_{12}$-(η^2-CH) and 2.0 ml of HSO_3CF_3 was prepared, evacuated and then warmed to room temperature. After three days noncondensible gases were removed. Low temperature adsorption was employed to separate CH_4 and CO from H_2. The yields of H_2 and CO/CH_4 mixture were determined by PVT measurements and quantitative gas phase IR: H_2, 0.10; CH_4, 0.03; CO, 0.36 moles per mole cluster.

(μ-H)$Fe_4(CO)_{12}(\eta^2$-$COCH_3$)

To a solution of ca. 0.37 g [PPN][$Fe_4(CO)_{12}(\mu^3$-$COCH_3$)] in 5 ml ether was added ca. 40 μl HSO_3CF_3. After removing the ether under vacuum, the product was dissolved in hexane, filtered, concentrated and cooled to yield small black crystals. ^{1}H NMR δ = 4.08 ppm, 3 H; —26.2 ppm, 1 H. IR (cyclohexane), 2085vw, 2046vs, 2020s, 1998s, 1990m, 1890w. Elemental analyses for C and H were satisfactory. Mass spec: The parent ion was observed at 603.7 (theoretical = 603.57) with consecutive loss of CO observed down to the Fe_4 core. A crystal of approximate dimensions 0.40 × 0.10 × 0.40 mm was sealed in a glass capillary and mounted on an automatic diffractometer. Unit cell dimensions (Table 1) were determined as described for compound I.

Crystallographic data reduction

The observed data were corrected for background, Lorentz and polarization

(Continued on p. 130)

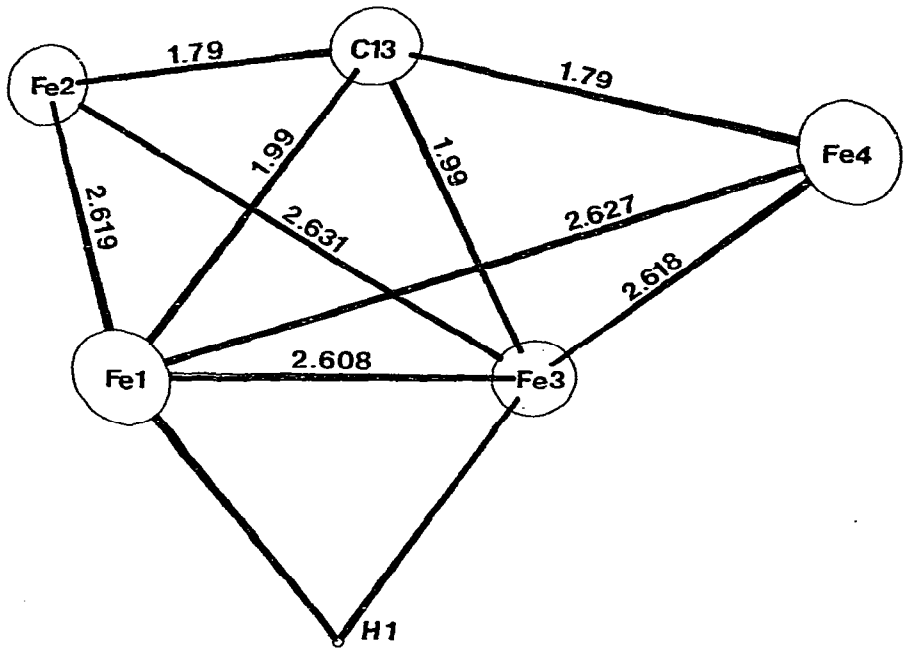

Fig. 1. Molecular structure of [PPN][(μ-H)$Fe_4(CO)_{12}C$]. Each iron is bonded to three carbonyls which have been omitted for clarity.

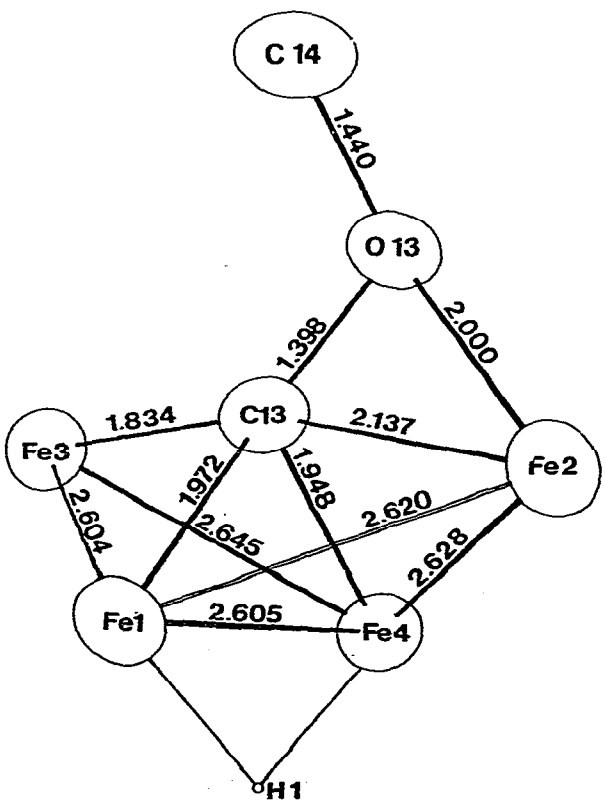

Fig. 2. Molecular structure of (μ-H)$Fe_4(CO)_{12}(\eta^2$-$COCH_3)$. Each iron is bonded to three carbonyls which have been omitted for clarity.

TABLE 2

BOND ANGLES (°) AND DISTANCES (Å) FOR $Fe_4C_{49}H_{31}NO_{12}P_2$ (II)

Fe(1)—Fe(4)	2.627(9)	C(1)—O(1)	1.14(6)
Fe(2)—Fe(4)	3.573(9)	C(2)—O(2)	1.15(6)
Fe(3)—Fe(4)	2.618(9)	C(3)—O(3)	1.15(6)
Fe(1)—Fe(3)	2.608(10)	C(4)—O(4)	1.14(6)
Fe(2)—Fe(3)	2.631(9)	C(5)—O(5)	1.16(6)
Fe(1)—Fe(2)		C(6)—O(6)	1.15(5)
		C(7)—O(7)	1.15(6)
C(13)—Fe(1)	1.99(4)	C(8)—O(8)	1.13(6)
C(13)—Fe(2)	1.79(5)	C(9)—O(9)	1.16(6)
C(13)—Fe(3)	1.99(4)	C(10)—O(10)	1.15(6)
C(13)—Fe(4)	1.79(5)	C(11)—O(11)	1.14(6)
		C(12)—O(12)	1.15(6)
H(1)—Fe(1)	1.62		
H(1)—Fe(3)	1.67	P(1)—N(1)	1.57(4)
		P(2)—N(1)	1.56(4)
Fe(1)—C(7)	1.76(5)	P(1)—C(101)	1.78(4)
Fe(1)—C(8)	1.78(5)	P(1)—C(201)	1.78(4)
Fe(1)—C(9)	1.76(4)	P(1)—C(301)	1.80(4)
Fe(2)—C(10)	1.81(5)	P(2)—C(401)	1.78(4)
Fe(2)—C(11)	1.76(5)	P(2)—C(501)	1.79(4)
Fe(2)—C(12)	1.75(5)	P(2)—C(601)	1.79(5)
Fe(3)—C(4)	1.78(5)		
Fe(3)—C(5)	1.76(5)		
Fe(3)—C(6)	1.75(4)		
Fe(4)—C(1)	1.76(5)		
Fe(4)—C(2)	1.76(5)		
Fe(4)—C(3)	1.80(5)		

Fe(2)—Fe(1)—Fe(4)	85.8(3)	C(7)—Fe(1)—Fe(2)	80(2)
Fe(3)—Fe(1)—Fe(4)	60.0(2)	C(7)—Fe(1)—Fe(3)	106(2)
Fe(2)—Fe(1)—Fe(3)	60.4(2)	C(7)—Fe(1)—Fe(4)	164(2)
Fe(2)—Fe(1)—C(13)	43(1)	C(7)—Fe(1)—C(13)	123(2)
Fe(4)—Fe(1)—H(1)	43(1)	C(8)—Fe(1)—Fe(2)	96(1)
Fe(2)—Fe(1)—H(1)	86	C(8)—Fe(1)—Fe(3)	142(1)
Fe(4)—Fe(1)—H(1)	88	C(8)—Fe(1)—Fe(4)	91(2)
Fe(3)—Fe(1)—C(13)	49(1)	C(8)—Fe(1)—C(13)	93(2)
Fe(2)—Fe(3)—Fe(4)	85.8(3)	C(9)—Fe(1)—Fe(2)	169(2)
Fe(4)—Fe(3)—Fe(1)	60.4(2)	C(9)—Fe(1)—Fe(3)	109(2)
Fe(2)—Fe(3)—Fe(1)	60.0(2)	C(9)—Fe(1)—Fe(4)	91(1)
Fe(2)—Fe(3)—C(13)	43(1)	C(9)—Fe(1)—C(13)	133(2)
Fe(4)—Fe(3)—C(13)	43(1)	C(7)—Fe(1)—C(8)	98(2)
Fe(2)—Fe(3)—H(1)	85	C(7)—Fe(1)—C(9)	101(2)
Fe(4)—Fe(3)—H(1)	87	C(8)—Fe(1)—C(9)	94(2)
Fe(1)—Fe(3)—C(13)	49(1)	C(4)—Fe(3)—Fe(2)	89(2)
Fe(1)—Fe(2)—Fe(3)	59.6(2)	C(4)—Fe(3)—Fe(1)	107(2)
Fe(3)—Fe(2)—C(13)	49(1)	C(4)—Fe(3)—Fe(4)	167(2)
Fe(1)—Fe(2)—C(13)	49(1)	C(4)—Fe(3)—C(13)	131(2)
Fe(1)—Fe(4)—Fe(3)	59.6(2)	C(5)—Fe(3)—Fe(2)	168(2)
Fe(3)—Fe(4)—C(13)	50(1)	C(5)—Fe(3)—Fe(1)	110(2)
Fe(1)—Fe(4)—C(13)	49(1)	C(5)—Fe(3)—Fe(4)	83(2)
Fe(3)—C(13)—Fe(2)	88(2)	C(5)—Fe(3)—C(13)	126(2)
Fe(1)—C(13)—Fe(2)	88(2)	C(6)—Fe(3)—Fe(2)	92(2)
Fe(3)—C(13)—Fe(4)	87(2)	C(6)—Fe(3)—Fe(1)	143(2)
Fe(1)—C(13)—Fe(4)	88(2)	C(6)—Fe(3)—Fe(4)	97(2)
Fe(1)—C(13)—Fe(3)	82(1)	C(6)—Fe(3)—C(13)	94(2)
Fe(2)—C(13)—Fe(4)	174(2)		

C(4)—Fe(3)—C(5)	101(2)	C(1)—Fe(4)—Fe(1)	151(2)
C(4)—Fe(3)—C(6)	95(2)	C(1)—Fe(4)—Fe(3)	94(2)
C(5)—Fe(3)—C(6)	94(2)	C(1)—Fe(4)—C(13)	105(2)

TABLE 2 (continued)

C(10)—Fe(2)—Fe(3)	101(2)	C(2)—Fe(4)—Fe(1)	102(2)
C(10)—Fe(2)—Fe(1)	108(2)	C(2)—Fe(4)—Fe(3)	152(2)
C(10)—Fe(2)—C(13)	148(2)	C(2)—Fe(4)—C(13)	102(2)
C(11)—Fe(2)—Fe(3)	153(2)	C(3)—Fe(4)—Fe(1)	98(1)
C(11)—Fe(2)—Fe(1)	96(2)	C(3)—Fe(4)—Fe(3)	105(2)
C(11)—Fe(2)—C(13)	107(2)	C(3)—Fe(4)—C(13)1	144(2)
C(12)—Fe(2)—Fe(3)	100(2)	C(1)—Fe(4)—C(2)	96(2)
C(12)—Fe(2)—Fe(1)	148(2)	C(1)—Fe(4)—C(3)	101(2)
C(12)—Fe(2)—C(13)	99(2)	C(2)—Fe(4)—C(3)	98(2)
C(10)—Fe(2)—C(11)	97(2)		
C(10)—Fe(2)—C(12)	100(2)		
C(11)—Fe(2)—C(12)	96(2)		

effects. The structures were solved by heavy atom methods and refinement of scale factor, positional and anisotropic thermal parameters for all non-hydrogen atoms reached $R = 3.1\%$ for compound I and $R = 3.6\%$ for compound II, where $R = \Sigma \| |F_o| - |F_c| \| / \Sigma |F_o| \times 100$. Figures 1 and 2 show structures of the cluster frameworks, based on the positional parameters of Tables 4 and 5. A table of final structure amplitudes is available along with related supplementary crystallographic data *.

Description of the crystal structures

Both [PPN][(μ-H)$Fe_4(CO)_{12}C$] (I) and (μ-H)$Fe_4(CO)_{12}(\eta^2$-$COCH_3)$ (II) exist in what is commonly referred to as a butterfly configuration which is an edge-shared bistriangular array of irons. To facilitate the discussion we refer to specific metal atoms by their connectivity to other metals in the cluster. Thus iron atoms at the wing tips of the butterfly are designated as c_{m2} and those at the hinge of the wings are c_{m3} (c_m designates metal connectivity and the numeral designates the number of metal atoms within bonding distance). Bond angles and distances are listed in Tables 2 and 3.

For I the hydride lies about 1.65 (av) Å from the two c_{m3} irons, a distance which is in the normal range seen for bridging metal hydrides. The carbide is bonded to all four iron atoms, being 1.99(4) Å from the c_{m3} irons and 1.79(5) Å from the c_{m2} irons. The dihedral angle discussed in this paper is defined by the intersection of the planes containing the 2 c_{m3} and 1 of the c_{m2} iron atoms and is 104° for I. The angle Fe(c_{m2})—C—Fe(c_{m2}) of 174(2)° shows that the carbide atom is slightly exposed.

Complex II can be viewed as the addition of a CH_3O^+ unit to I where the oxygen bridges a C—Fe(c_{m2}) bond in the same fashion observed for H^+ in (μ-H)-$Fe_4(CO)_{12}(\eta^2$-CH) [3]. The $COCH_3{}^+$ ligand contributes a total of 4 electrons to the cluster framework. The Fe—O distance is 2.000(1) Å and is well within bonding range. The hydride again bridges the two c_{m3} irons at an average distance of 1.69 Å.

* Supplementary material has been deposited as a NAPS document. Order from NAPS c/o Microfiche Publications, P.O. Box 513, Grand Central Station, New York, N.Y. 10017.

TABLE 3

BOND ANGLES (°) AND DISTANCES (Å) FOR $Fe_4C_{14}H_4O_{13}$

Fe(1)—Fe(4)	2.605(1)	C(4)—O(4)	1.131(3)
Fe(2)—Fe(4)	2.628(1)	C(5)—O(5)	1.144(2)
Fe(3)—Fe(4)	2.645(1)	C(6)—O(6)	1.112(2)
Fe(1)—Fe(3)	2.604(1)	C(7)—O(7)	1.134(2)
Fe(1)—Fe(2)	2.620(1)	C(8)—O(8)	1.133(2)
C(13)—Fe(1)	1.972(2)	C(9)—O(9)	1.140(3)
C(13)—Fe(2)	2.137(2)	C(10)—O(10)	1.145(2)
C(13)—Fe(3)	1.834(2)	C(11)—O(11)	1.136(2)
C(13)—Fe(4)	1.948(2)	C(12)—O(12)	1.131(4)
H(1)—Fe(1)	1.64	C(13)—O(13)	1.398(2)
H(1)—Fe(4)	1.74	C(14)—O(13)	1.440(2)
Fe(1)—C(1)	1.792(2)	C(14)—H(2)	0.93
Fe(1)—C(2)	1.806(2)	C(14)—H(3)	1.01
Fe(1)—C(3)	1.770(2)	C(14)—H(4)	0.97
Fe(2)—C(4)	1.803(2)	O(13)—Fe(2)	2.000(2)
Fe(2)—C(5)	1.753(2)	Fe(3)—Fe(1)—Fe(4)	61.05(2)
Fe(2)—C(6)	1.841(2)	Fe(3)—Fe(1)—Fe(2)	97.42(3)
Fe(3)—C(10)	1.755(1)	Fe(4)—Fe(1)—Fe(2)	60.39(2)
Fe(3)—C(11)	1.833(2)	Fe(1)—Fe(2)—Fe(4)	59.53(2)
Fe(3)—C(12)	1.782(3)	Fe(1)—Fe(3)—Fe(4)	59.50(2)
Fe(4)—C(7)	1.803(2)	Fe(1)—Fe(4)—Fe(2)	60.08(2)
Fe(4)—C(8)	1.782(2)	Fe(1)—Fe(4)—Fe(3)	59.45(2)
Fe(4)—C(9)	1.799(2)	Fe(2)—Fe(4)—Fe(3)	96.19(2)
C(1)—O(1)	1.150(2)	H(1)—Fe(1)—Fe(3)	90
C(2)—O(2)	1.131(2)	H(1)—Fe(2)—Fe(4)	41
C(3)—O(3)	1.152(3)	H(1)—Fe(1)—Fe(2)	81
H(1)—Fe(4)—Fe(1)	38	C(1)—Fe(1)—Fe(3)	67.05(5)
H(1)—Fe(4)—Fe(2)	79	C(2)—Fe(1)—Fe(3)	154.5(1)
H(1)—Fe(4)—Fe(3)	86	C(3)—Fe(1)—Fe(3)	104.4(1)
C(13)—Fe(1)—Fe(3)	44.66(5)	C(1)—Fe(1)—Fe(4)	106.5(1)
C(13)—Fe(1)—Fe(4)	47.95(7)	C(2)—Fe(1)—Fe(4)	114.0(1)
C(13)—Fe(1)—Fe(2)	53.25(5)	C(3)—Fe(1)—Fe(4)	142.5(1)
C(13)—Fe(2)—Fe(1)	47.65(4)	C(1)—Fe(1)—C(13)	111.6(1)
C(13)—Fe(2)—Fe(4)	46.86(6)	C(2)—Fe(1)—C(13)	152.3(1)
C(13)—Fe(3)—Fe(1)	49.08(4)	C(3)—Fe(1)—C(13)	96.46(7)
C(13)—Fe(4)—Fe(1)	48.73(4)	C(1)—Fe(1)—C(2)	92.90(7)
C(13)—Fe(4)—Fe(2)	53.21(5)	C(1)—Fe(1)—C(3)	96.91(9)
C(13)—Fe(4)—Fe(3)	43.87(5)	C(2)—Fe(1)—C(3)	93.04(8)
C(13)—O(13)—C(14)	119.5(1)	C(4)—Fe(2)—Fe(1)	104.5(1)
C(13)—O(13)—Fe(2)	75.64(9)	C(5)—Fe(2)—Fe(2)	83.92(6)
O(13)—Fe(2)—Fe(1)	81.97(4)	C(6)—Fe(2)—Fe(1)	156.4(1)
O(13)—Fe(2)—Fe(4)	76.74(4)	C(4)—Fe(2)—Fe(4)	163.8(1)
C(14)—O(13)—Fe(2)	129.4(1)	C(5)—Fe(2)—Fe(4)	90.09(6)
O(13)—C(13)—Fe(1)	130.1(1)	C(6)—Fe(2)—Fe(4)	97.04(8)
O(13)—C(13)—Fe(2)	65.04(9)	C(4)—Fe(2)—C(13)	121.5(1)
O(13)—C(13)—Fe(3)	132.6(1)	C(5)—Fe(2)—C(13)	124.9(1)
O(13)—C(13)—Fe(4)	120.3(1)	C(6)—Fe(2)—C(13)	119.7(1)
C(1)—Fe(1)—Fe(2)	164.0(1)	C(4)—Fe(2)—O(13)	99.55(7)
C(2)—Fe(1)—Fe(2)	100.8(1)	C(5)—Fe(2)—O(13)	165.2(1)
C(3)—Fe(1)—Fe(2)	90.55(5)	C(6)—Fe(2)—O(13)	96.39(7)
C(4)—Fe(2)—C(5)	90.71(8)	C(7)—Fe(4)—C(13)	141.1(1)
C(4)—Fe(2)—C(6)	99.04(9)	C(8)—Fe(4)—C(13)	90.61(8)
C(5)—Fe(2)—C(6)	93.73(9)	C(9)—Fe(4)—C(13)	124.0(1)
C(10)—Fe(3)—Fe(1)	144.3(1)	C(7)—Fe(4)—C(8)	94.24(8)
C(11)—Fe(3)—Fe(1)	113.9(1)	C(7)—Fe(4)—C(9)	93.66(11)
C(12)—Fe(3)—Fe(1)	96.16(5)	C(8)—Fe(4)—C(9)	97.30(7)
C(10)—Fe(3)—Fe(4)	98.09(7)		
C(11)—Fe(3)—Fe(4)	106.9(1)		
C(12)—Fe(3)—Fe(4)	150.3(1)		
C(10)—Fe(3)—C(13)	95.22(7)		

TABLE 3 (continued)

C(11)—Fe(3)—C(13)	152.6(1)
C(12)—Fe(3)—C(13)	104.5(1)
C(10)—Fe(3)—C(11)	98.52(7)
C(10)—Fe(3)—C(12)	93.36(9)
C(11)—Fe(3)—C(12)	98.29(12)
C(7)—Fe(4)—Fe(1)	113.7(1)
C(8)—Fe(4)—Fe(1)	139.0(1)
C(9)—Fe(4)—Fe(1)	109.6(1)
C(7)—Fe(4)—Fe(2)	87.92(8)
C(8)—Fe(4)—Fe(2)	93.41(6)
C(9)—Fe(4)—Fe(2)	169.0(1)
C(7)—Fe(4)—Fe(3)	167.6(1)
C(8)—Fe(4)—Fe(3)	97.18(7)
C(9)—Fe(4)—Fe(3)	80.12(8)

TABLE 4

POSITIONAL PARAMETERS FOR $Fe_4C_{49}H_{31}NO_{12}P_2$ (I)

Atom	$x(\sigma(x))$	$y(\sigma(y))$	$z(\sigma(z))$	Atom	$x(\sigma(x))$	$y(\sigma(y))$	$z(\sigma(z))$
Fe(1)	0.6588(5)	0.2552(5)	0.2573(4)	C(103)	0.072(5)	0.400(4)	0.030(3)
Fe(2)	0.5210(6)	0.2084(5)	0.1264(4)	C(104)	0.184(5)	0.429(4)	0.048(3)
Fe(3)	0.4788(5)	0.3384(5)	0.2490(4)	C(105)	0.263(4)	0.396(4)	—0.005(3)
Fe(4)	0.4840(5)	0.1830(5)	0.3526(4)	O(106)	0.229(4)	0.337(4)	0.922(3)
C(1)	0.338(4)	0.158(4)	0.371(3)	C(201)	0.175(3)	0.266(3)	0.729(2)
C(2)	0.504(4)	0.054(4)	0.373(3)	C(202)	0.226(4)	0.191(3)	0.687(3)
C(3)	0.536(4)	0.244(4)	0.453(3)	C(203)	0.298(4)	0.220(4)	0.619(3)
C(4)	0.508(4)	0.443(4)	0.175(3)	C(204)	0.320(4)	0.322(4)	0.592(3)
C(5)	0.464(4)	0.409(4)	0.345(3)	C(205)	0.274(4)	0.396(4)	0.636(3)
C(6)	0.334(4)	0.308(4)	0.226(3)	C(206)	0.202(4)	0.369(3)	0.703(3)
C(7)	0.747(4)	0.312(4)	0.175(3)	C(301)	0.056(3)	0.094(3)	0.832(3)
C(8)	0.702(4)	0.131(4)	0.259(3)	C(302)	0.111(4)	0.062(4)	0.901(3)
C(9)	0.738(4)	0.306(4)	0.349(3)	C(303)	0.095(5)	—0.044(5)	0.918(4)
C(10)	0.570(5)	0.299(4)	0.042(3)	C(304)	0.026(5)	—0.114(4)	0.866(5)
C(11)	0.580(4)	0.103(4)	0.086(3)	C(305)	—0.028(5)	—0.083(4)	0.796(4)
C(12)	0.384(4)	0.158(4)	0.089(3)	C(306)	—0.013(4)	0.021(4)	0.779(4)
C(13)	0.498(3)	0.190(3)	0.238(3)	C(401)	0.730(4)	0.247(4)	0.752(3)
O(1)	0.243(3)	0.142(3)	0.380(3)	C(402)	0.704(4)	0.162(4)	0.804(4)
O(2)	0.513(3)	—0.031(2)	0.386(2)	C(403)	0.596(5)	0.131(5)	0.835(4)
O(3)	0.572(3)	0.283(3)	0.518(2)	C(404)	0.514(5)	0.186(6)	0.314(4)
O(4)	0.525(3)	0.513(3)	0.131(2)	C(405)	0.537(4)	0.270(5)	0.763(4)
O(5)	0.450(3)	0.460(3)	0.405(2)	C(406)	0.646(4)	0.301(4)	0.729(3)
O(6)	0.239(2)	0.289(3)	0.211(2)	C(501)	0.870(4)	0.201(3)	0.612(3)
O(7)	0.812(3)	0.350(4)	0.125(2)	C(502)	0.774(4)	0.138(4)	0.578(3)
O(8)	0.729(3)	0.053(3)	0.261(2)	C(503)	0.779(5)	0.079(4)	0.504(4)
O(9)	0.792(3)	0.343(3)	0.407(2)	C(504)	0.878(6)	0.081(4)	0.463(3)
O(10)	0.601(4)	0.354(3)	—0.012(2)	C(505)	0.975(4)	0.143(4)	0.494(3)
O(11)	0.607(3)	0.033(3)	0.062(2)	C(506)	0.971(4)	0.203(4)	0.568(3)
O(12)	0.293(3)	0.120(3)	0.069(3)	C(601)	0.896(4)	0.413(3)	0.680(3)
P(2)	0.8687(10)	0.2778(9)	0.7089(7)	C(602)	0.943(4)	0.489(4)	0.740(3)
P(1)	0.0690(10)	0.2319(9)	0.8079(7)	C(603)	0.961(4)	0.595(4)	0.722(4)
N(1)	0.951(3)	0.255(3)	0.780(2)	C(604)	0.932(5)	0.624(4)	0.642(4)
C(101)	0.115(3)	0.308(3)	0.902(3)	C(605)	0.884(6)	0.550(5)	0.582(4)
C(102)	0.037(4)	0.340(4)	0.957(3)	C(606)	0.866(5)	0.444(4)	0.600(3)

TABLE 5

POSITIONAL PARAMETERS FOR $Fe_4C_{14}H_4O_{13}$ (II)

Atom	x(σ(x))	y(σ(y))	z(σ(z))
Fe(1)	0.35118(3)	0.05960(3)	0.17040(2)
Fe(2)	0.59406(3)	0.39389(3)	0.17034(2)
Fe(3)	0.43309(3)	0.10491(3)	0.35390(2)
Fe(4)	0.37250(3)	0.31710(3)	0.27921(2)
C(1)	0.2020(2)	−0.1410(2)	0.2050(1)
C(2)	0.1956(2)	−0.0278(2)	0.0524(1)
C(3)	0.4878(2)	−0.0009(2)	0.1322(1)
C(4)	0.7194(2)	0.3806(2)	0.0911(1)
C(5)	0.4210(2)	0.3475(2)	0.0736(1)
C(6)	0.0790(3)	0.6381(2)	0.1998(1)
C(7)	0.2830(3)	0.4169(2)	0.2150(1)
C(8)	0.5397(2)	0.5191(2)	0.3709(1)
C(9)	0.1939(3)	0.2222(2)	0.3383(1)
C(10)	0.5899(2)	0.2604(2)	0.4638(1)
C(11)	0.2348(3)	−0.0412(3)	0.3970(1)
C(12)	0.5264(3)	−0.0194(2)	0.3552(1)
C(13)	0.5469(2)	0.2589(2)	0.2811(1)
C(14)	0.8633(2)	0.3529(2)	0.3035(1)
O(1)	0.0932(2)	−0.2864(2)	0.2062(1)
O(2)	0.0949(2)	−0.0901(2)	−0.0210(1)
O(3)	0.5720(2)	−0.0452(2)	0.1059(1)
O(4)	0.7955(3)	0.3735(2)	0.0395(1)
O(5)	0.3167(2)	0.3257(2)	0.0086(1)
O(6)	0.7775(2)	0.7853(2)	0.2155(1)
O(7)	0.2252(2)	0.4822(2)	0.1786(1)
O(8)	0.6487(2)	0.6453(2)	0.4300(1)
O(9)	0.0742(2)	0.1706(2)	0.3711(1)
O(10)	0.6984(2)	0.3629(2)	0.5333(1)
O(11)	0.1162(2)	−0.1329(2)	0.4261(1)
O(12)	0.5882(2)	−0.0959(2)	0.3531(1)
O(13)	0.7320(1)	0.3936(1)	0.2902(1)
H(1)	0.2280	0.1352	0.1792
H(2)	0.9766	0.4565	0.3053
H(3)	0.8813	0.3712	0.3743
H(4)	0.8320	0.2558	0.2515

Discussion

Complexes I and II are two examples of the increasing number of iron butterfly complexes. The general Fe_4 array also is observed for $[Me_3NCH_2Ph][(\mu\text{-H})Fe_4(CO)_{12}(\eta^2\text{-CO})]$ (III) [5], $[Zn(NH_3)_4][Fe_4(CO)_{12}C]$ (IV) [6], $(\mu\text{-H})Fe_4(CO)_{12}(\eta^2\text{-CH})$ (V) [3], $Fe_4(CO)_{13}C$ (VI) [7] and $[Et_4N][Fe_4(CO)_{12}(CCO_2CH_3)]$ (VII) [8]. Each iron is bonded to three terminal carbonyls, which have been omitted in structures I—VII. The complex I is the intermediate stage in protonation of the dianion $[Fe_4(CO)_{12}C]^{2-}$ to $(\mu\text{-H})Fe_4(CO)_{12}(\eta^2\text{-CH})$. Compounds I and VI belong to the class of electron-saturated 62-electron butterfly clusters [9]. On the other hand, $[Fe_4(CO)_{12}(CC(O)OCH_3)]^-$ (VII) is only a 60-electron system and would be predicted by theory to prefer a tetrahedral geometry. The considerably shorter iron—iron bond distances in this complex [2.47 Å (av) vs > 2.6 Å for I—VI] implies the possibility of partial multiple metal—metal bonding, delocalized over the Fe_4 framework. (Localized bond

contraction is the electron-deficient $H_2Os_3(CO)_{10}$ has been observed and an osmium—osmium double bond is proposed [10].)

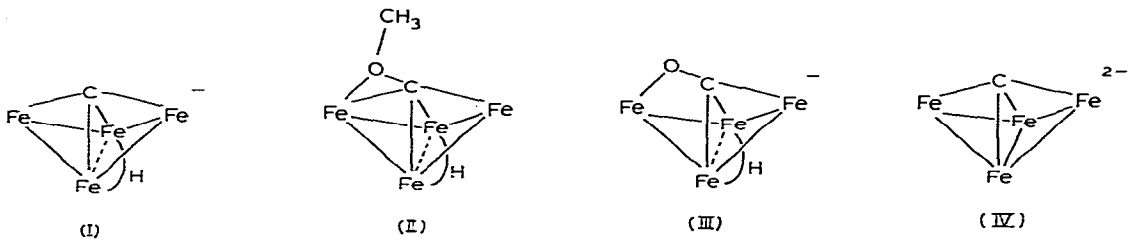

(I) (II) (III) (IV)

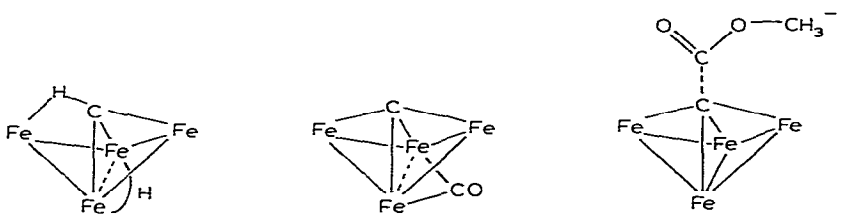

(V) (VI) (VII)

In $Fe_4(CO)_{13}^{2-}$ the μ_3-C—O bond is 1.20 Å [11], which lengthens to 1.26 Å on the formation of η^2-CO in $HFe_4(CO)_{13}^-$. The attachment of a CH_3^+ to the oxygen of this η^2-CO results in a much greater lengthening of the CO bond to 1.39 Å In addition, alkylation of the CO oxygen shortens the average C—Fe distance from 2.05 Å in $HFe_4(CO)_{13}^-$ to 1.97 Å in $HFe_4(CO)_{12}(\eta^2$-COMe). In this way the electron acceptor on oxygen and the metal framework appear to act in concert to weaken the CO bond. As will be discussed below, the strong acid medium is likely to generate a species $HFe_4(CO)_{12}(\mu^2$-COH) in which the CO is activated in a manner analogous to that found for $HFe(CO)_{12}(\eta^2$-COMe).

There are several other structural features which deserve comment before returning to the mechanism of CO activation. A remarkable observation in all six of the 62 electron four-iron butterfly compounds is that the average Fe—Fe distance is virtually constant (2.622 ± 0.002 Å). The average Fe—Fe bond length is maintained despite changes in Fe—ligand and even individual Fe—Fe bond lengths. The largest variation in Fe—Fe distance is observed when the Fe(c_{m3})—Fe(c_{m3}) bond is protonated. For example, this distance is 2.53 Å in $Fe_4(CO)_{12}C^-$ [2] and 2.61 Å in $HFe_4(CO)_{12}C^-$. Similarly this hydride-bridged Fe—Fe distance is virtually constant for the iron butterfly compounds having this structural feature: $HFe_4(CO)_{12}(CH)$, 2.6053(8); $HFe_4(CO)_{12}C^-$, 2.608(10); $HFe_4(CO)_{12}(COCH_3)$, 2.605(1) Å. Finally, we note that the dihedral angle between the two Fe_3 triangles increases from $HFe_4(CO)_{12}(C)^-$, 104°, to $HFe_4(CO)_{12}(COCH_3)$, 119°; so the butterfly array appears to be highly compliant to variations in ligand bonding and steric requirements. This flapping motion of the butterfly may facilitate the conversion of η^2-CO to CH_4 described below.

As outlined in the Experimental section, the proton-induced reduction of $Fe_4(CO)_{13}^{2-}$ was quenched after one hour of reaction at room temperature, by

extraction of metal cluster compounds into a hydrocarbon phase. The species in the hydrocarbon extract was found to be $HFe_4(CO)_{12}(\eta^2\text{-CH})$ by ^1H NMR. Removal of the hydrocarbon solvent and recrystallization from methanol yielded [PPN][$HFe(CO)_{12}C$], for which the crystal structure is described above. Thus the carbide cluster is not a principal species in the acid reaction mixture, but rather an artifact of the use of a mildly basic solvent for the recrystallization of the product.

The possible intermediacy of $HFe_4(CO)_{12}(\eta^2\text{-CH})$ in the proton-induced reduction was further tested by the reaction of this cluster with HSO_3CF_3 and collection of the gaseous products. Methane was indeed produced but the yield was small by comparison with that of the usual proton-induced reaction. Thus it is possible that $HFe_4(CO)_{12}(CH)$ is a reactive intermediate but some of the other species in solution must influence its conversion to methane.

The observed conversion of $HFe_4(CO)_{13}^-$ to $HFe_4(CO)_{12}(\eta^2\text{-CH})$ in strong acid provides a homogeneous parallel to the activation of CO on a Ni surface, where the CO is cleaved to produce an active surface carbide, which subsequently is reduced [12]. The exact route by which the CO in $HFe_4(CO)_{13}^-$ is cleaved must be somewhat complicated.

As the first step, this anion probably is converted to $H_2Fe_4(CO)_{13}$, which was originally reported by Hieber, but which has not been completely characterized [13]. In nonbasic solvents the addition of one equivalent of strong acid converts $HFe_4(CO)_{13}^-$ into a material which has the general characteristics described by Hieber and which has IR and low temperature ^{13}C NMR which are compatible with $H_2Fe_4(CO)_{13}$. However, when $HFe_4(CO)_{13}^-$ is dissolved in HSO_3CF_3 an IR spectrum in the CO stretching region is obtained which compares in its major features with the spectrum obtained from $HFe_4(CO)_{12}(\eta^2\text{-CH})$ dissolved in this strong acid. Furthermore, the individual CO stretching bands of $HFe_4(\eta^2\text{-CO})_{12}(CH)$ are shifted some 40 cm^{-1} to higher frequency in this strong acid, indicating that this species has been protonated, perhaps at the remaining $Fe(c_{m2})$—C bond, to produce VIII. The conversion of $HFe_4(CO)_{13}^-$ to V or VIII requires two electrons. We presently suppose that these reducing equivalents are supplied by electron transfer from other organometallic species in solution.

In summary, the present results provide evidence for the proton cleavage of an η^2-CO in acid solution, and the structural data indicate that the metal cluster facilitates this cleavage process by forming a tighter bond with the C atom as the oxygen leaves. Our current information and speculations on the course of the proton-induced reduction of CO in this four-iron cluster system are summarized in Scheme 2. The first step to produce III involves a well established transformation [5]. Step 2 produces $H_2Fe_4(CO)_{13}$ which has been reported previously [12]. We write the indicated structure by analogy with the structure of II, and this structure is consistent with our spectroscopic data. Based on the structural data for compound II, the protonation of the CO oxygen in step 2 activates CO by lengthening the CO bond and increasing the C—cluster interactions. The details of steps 3 are lacking; however, the combination of steps 3 and 4 can be inferred by the extraction of V from the reaction mixture. The protonation of V to produce VIII is inferred from the increase in terminal CO stretching frequencies of V in HSO_3CF_3 solution, but of course the exact struc-

SCHEME 2

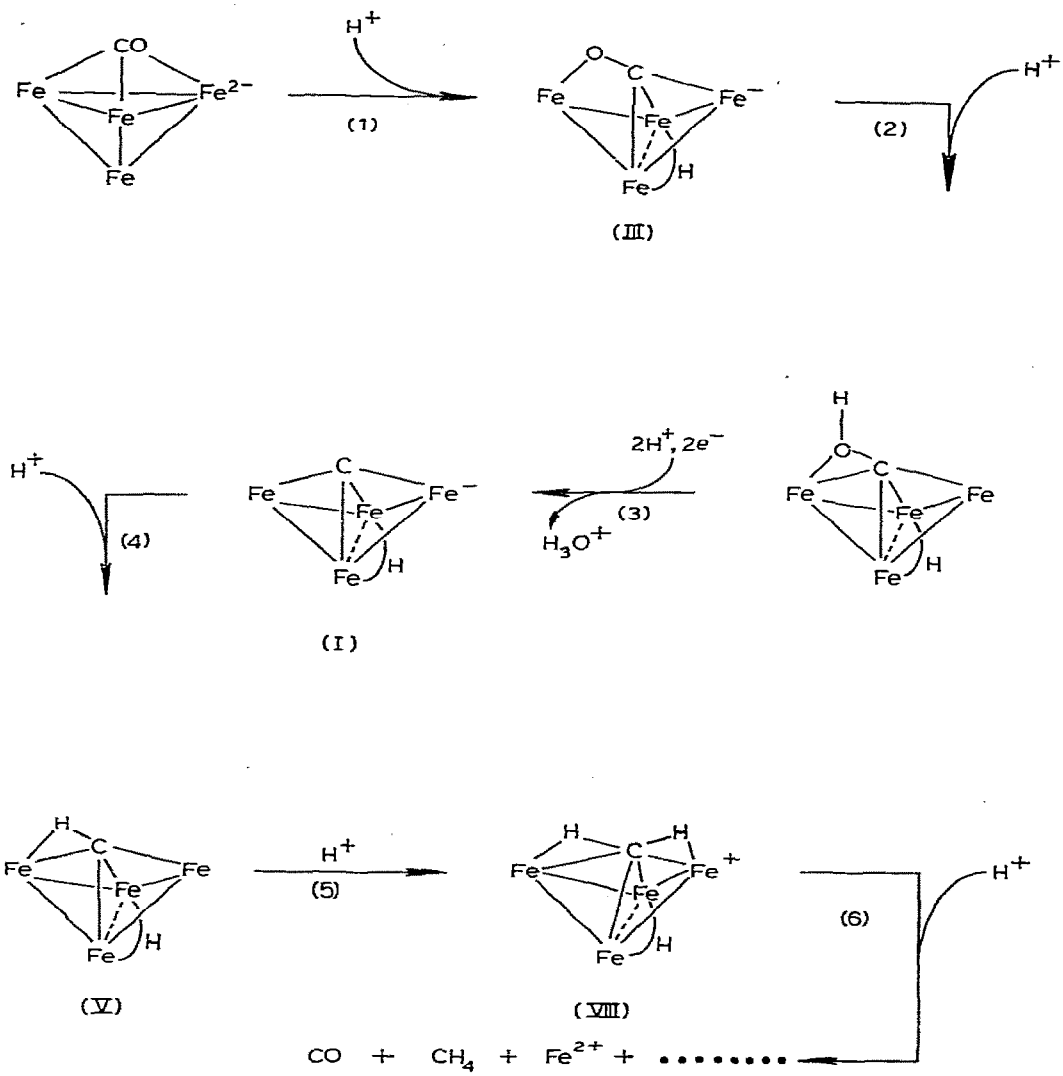

ture is a matter of speculation. The sequence of events involved in reaction 6 for the production of methane from the proposed methylene center, are currently being investigated.

Acknowledgments

The portion of this research which was conducted at Northwestern University was sponsored by the NSF synthetic organometallic program. We appreciate the helful exchange of data with Prof. E.L. Muetterties, Dr. J. Williams, Dr.

J. Bradley, Dr. M. Manassero, and the late Professor Paolo Chini. We also thank Drs. J.A. Bertrand and D.G. van Derveer for the use of the diffractometer at Georgia Institute of Technology, and for their kind assistance.

References

1 K. Whitmire and D.F. Shriver, J. Amer. Chem. Soc., 102 (1980) 1456.
2 K. Whitmire, D.F. Shriver and E.M. Holt, J. Chem. Soc., Chem. Commun., (1980) 780.
3 M. Tachikawa and E.L. Muetterties, J. Amer. Chem. Soc., 102 (1980) 4541.
4 M.A. Beno, J.M. Williams, M. Tachikawa and E.L. Muetterties, J. Amer. Chem. Soc., 102 (1980) 4542.
5 M. Manassero, M. Sansoni and G. Longoni, J. Chem. Soc., J. Chem. Soc. Chem. Commun., (1976) 919.
6 J.H. Davis, M.A. Beno, J.M. Williams, J. Zimmie, M. Tachikawa and E.L. Muetterties, private communication.
7 J.S. Bradley, private communication.
8 J.S. Bradley, G.B. Ansell and E.W. Hill, J. Amer. Chem. Soc., 101 (1979) 7417.
9 J.W. Lauher, J. Amer. Chem. Soc., 100 (1978) 5305.
10 R. Mason, Pure Appl. Chem., 33 (1973) 513.
11 R.J. Dodens and L.F. Dahl, J. Amer. Chem. Soc., 88 (1966) 4847.
12 S.V. Ho and P. Harriot, J. Catal., 64 (1980) 272.
13 W. Hieber and R. Werner, Chem. Ber., 90 (1957) 286.